Frequency-Comb Based Double-Quantum Two-Dimensional Spectrum Identifies Collective Hyperfine Resonances in Atomic Vapor Induced by Dipole-Dipole Interactions

Bachana Lomsadze and Steven T. Cundiff*
Department of Physics, University of Michigan, Ann Arbor, Michigan 48109, USA

(Received 9 November 2017; published 8 June 2018)

Frequency-comb based multidimensional coherent spectroscopy is a novel optical method that enables high-resolution measurement in a short acquisition time. The method's resolution makes multidimensional coherent spectroscopy relevant for atomic systems that have narrow resonances. We use double-quantum multidimensional coherent spectroscopy to reveal collective hyperfine resonances in rubidium vapor at 100 °C induced by dipole-dipole interactions. We observe tilted and elongated line shapes in the double-quantum 2D spectra, which have never been reported for Doppler-broadened systems. The elongated line shapes suggest that the signal is predominately from the interacting atoms that have a near zero relative velocity.

DOI: 10.1103/PhysRevLett.120.233401

Dipole-dipole interactions are among the most fundamental and important processes in atomic, molecular, and optical physics. Understanding these interactions is crucial, because they govern the physical mechanisms of many phenomena. Dipole-dipole interactions result in energy transfer between atoms, molecules, and complex biological systems [1–3]. They play the major role for the formation of homonuclear, heteronuclear, and exotic molecules [4]. These interactions are also critical for many applications such as quantum computing, Rydberg blockades, and designing single-quantum emitters [5–7].

Since its development over two decades ago, optical multidimensional coherent spectroscopy (MDCS) [8,9] has proven to be a powerful optical method for probing weak many-body interactions. It is an optical analog of multidimensional nuclear magnetic resonance spectroscopy [10] that has been a workhorse for several decades for determining the molecular structure. Optical MDCS is a nonlinear technique that uses a sequence of ultrafast laser pulses (typically, three) incident to the sample and records a nonlinear [four-wave-mixing (FWM)] signal emitted by the sample as a function of the time delay(s) between the incident pulses. A multidimensional spectrum is constructed by calculating the Fourier transforms of the emitted signal with respect to the emission time and the delays between the pulses. Depending on the time ordering of the excitation pulses, a multidimensional spectrum can give insight about many-body interactions and provide important spectroscopic information. For instance, if the photon-echo excitation sequence [11] is used, when the first pulse is a complex phase-conjugated pulse, a multidimensional spectrum (referred to as a single-quantum 2D spectrum) shows the couplings between the excited states, and it also differentiates the homogenous and inhomogeneous linewidths. Single-quantum spectra can also be used for chemical sensing applications to determine the constituent species in a mixture [12]. If the complex conjugated pulse arrives last, then the corresponding 2D spectrum (referred to as a double-quantum spectrum) can identify weak many-body interactions [13,14]. Until this point, however, due to the resolution and acquisition-speed limitations, MDCS techniques have mostly been used for systems that have broad resonances or fast dephasing rates (tens of femtoseconds to hundreds of picoseconds). They have not been able to probe fundamental processes such as the dipole-dipole interactions in atomic systems (with nanosecond or tens of nanoseconds dephasing times) that are the building blocks for complex matter.

Previously, single- and double-quantum MDCS measurements have been applied to rubidium (Rb) and potassium (K) atomic vapors (at 130 °C) to investigate collective resonances (collective excitation of multiple atoms) induced by weak dipole-dipole interactions [15,16]. However, due to limited spectrometer resolution, an argon (Ar) buffer gas was introduced into the vapor cell to artificially broaden the resonances to match the spectrometer resolution. The broadening led to the modification (distortion) of the natural Doppler-broadened line shapes. It is important to emphasize that obtaining undistorted line shapes is extremely critical, as the line shapes provide insight about the underlying physics of the many-body interactions. In addition, the experimental measurements [15,16] could not differentiate homonuclear (between same isotopes) and heteronuclear (between different isotopes) interactions. Collective resonances in a dilute potassium vapor were also studied by Bruder, Binz, and Stienkemeier [17] and theoretically explained by Mukamel [18]; however, the detected signal was due to noninteracting atoms

and, hence, contained no information about the dipole-dipole interactions.

Recently, we introduced a novel approach [12,19] to multidimensional coherent spectroscopy that utilizes frequency combs and the dual-comb detection technique [20,21]. This combination allowed us to demonstrate rapid single-quantum two-dimensional coherent spectroscopy with unprecedented resolution (hundreds of megahertz) [12]. Here, we take advantage of the speed and resolution achievable with the technique and extend its applications to double-quantum MDCS, investigating dipole-dipole interactions in atomic vapor. We apply our method to a vapor of Rb atoms containing both isotopes ^{87}Rb and ^{85}Rb at their natural abundance with Doppler-broadened features (at 100 °C) and observe collective hyperfine resonances (both homonuclear and heteronuclear) induced by weak dipole-dipole interactions. Our results also reveal that the FWM signal, due to many-body interactions, is stronger for the atoms that have a near zero relative velocity.

The experimental setup is shown in Fig. 1(a) with further details available in Refs. [12,22]. We used two homebuilt Kerr-lens mode-locked Ti:sapphire lasers centered at 800 nm. The repetition frequencies for the signal and the LO combs ($f_{\mathrm{rep}_{-\mathrm{sig}}} = 93.581\,904$ MHz and $f_{\mathrm{rep}_{-\mathrm{LO}}} = f_{\mathrm{rep}_{-\mathrm{sig}}} - 641$ Hz) were phase locked to a direct digital synthesizer, but the comb offset frequencies were not actively stabilized. The phase fluctuations due to fluctuations in the offset frequency, optical path length, and/or repetition frequency were measured and corrected using a scheme described in Refs. [12,22], which is similar to the phase correction schemes that are used in linear dual-comb spectroscopy [23–25]. The output of the signal comb was split into two parts. One part of the beam was frequency shifted by 80 MHz using an acousto-optical modulator and combined with the other part whose delay was controlled with the retroreflector mounted on a mechanical stage. The combined beams then were focused to 5 μm spot in a 0.5 mm thin vapor cell containing ^{87}Rb and ^{85}Rb atoms (at 100 °C). Before focusing, the beams were filtered with an optical bandpass filter centered at 794 nm (3 nm FWHM) to excite only the D_1 lines of both isotopes. Average powers per beam were 2.4 and 1.2 mW, respectively (after the

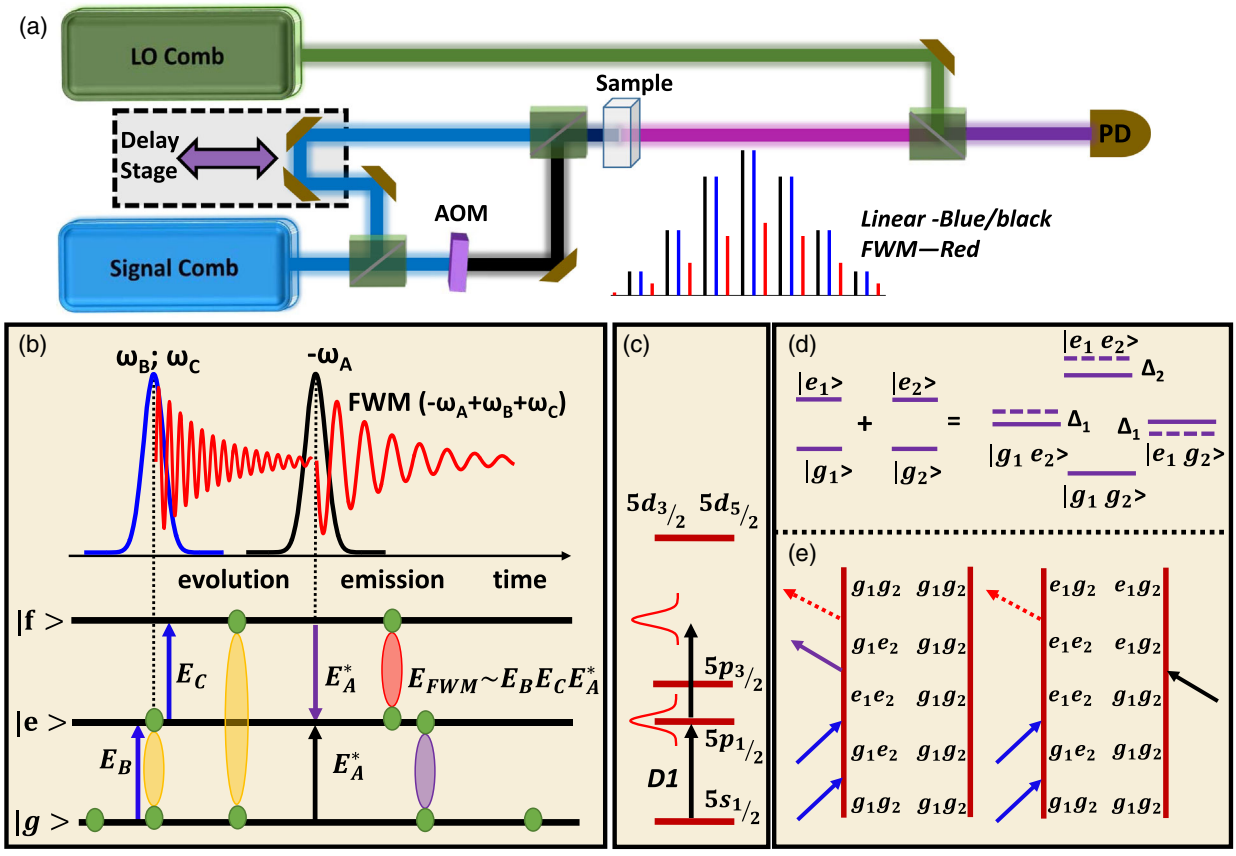

FIG. 1. (a) Schematic diagram of the experimental setup. AOM, acousto-optical modulator. PD, photodetector. The comb structure shown corresponds to linear (blue and black) and four-wave-mixing (red) comb lines in the frequency domain. (b) Time domain picture of FWM signal generation. $|g\rangle$, $|e\rangle$, and $|f\rangle$ correspond to ground, excited, and doubly excited states, respectively. (c) Fine structure of Rb atoms, showing no energy level at $2 \times D_1$ frequency. (d) Energy level diagram of two combined atoms without interactions. Dashed lines show the energy levels with interactions. (e) Double-sided Feynman diagrams of the double-quantum FWM signals.

filter). The generated FWM signal comb, along with the excitation combs, was then combined with the LO comb with a slightly different repetition rate and interfered on a photodetector. The output of the photodetector was spectrally filtered in the rf domain to isolate the FWM signal and digitized [22]. The delay between the excitation pulses was varied (over 1 ns that corresponds to < 900 MHz spectral resolution for our experiment) to generate the second dimension for the double-quantum two-dimensional spectrum.

The generation of a double-quantum FWM signal in the time domain with a pair of pulses is pictorially shown in Fig. 1(b). The first pulse (shown in blue) excites a coherence between the ground and singly excited states and then converts this coherence into the double-quantum coherence between the ground state and doubly excited state that evolves in time (the red trace in the figure shows the evolution of the coherence in time) [26]. Pulse A (complex-conjugate pulse shown in black) converts this coherence either back to the coherence between the ground and the excited state or to the coherence between the excited and doubly excited states that radiates the FWM signal (red trace in the figure). As mentioned earlier, the excitation beams in our experiment were optically filtered to excite only D_1 lines of Rb atoms, and there are no doubly excited states in Rb within the filtered bandwidth at $2 \times D_1$ frequency [see Fig. 1(c)]. In this case, the only way to obtain the double-quantum FWM signal is to consider a combined atom picture that clearly shows the doubly excited state [Fig. 1(d)]. In Fig. 1(e), we plot the double-sided Feynman diagrams [27] for the combined atom picture that would give rise to the FWM signal. However, the Feynman diagrams have opposite signs, and, since $|g_1 e_2\rangle - |g_1 g_2\rangle$ and $|e_1 e_2\rangle - |e_1 g_2\rangle$ transition energies are equal to each other, these double-sided Feynman diagrams perfectly cancel each other. The picture changes if we include the many-body interactions, particularly the dipole-dipole interactions [13,14]. In the presence of the interactions, the singly and doubly excited states experience slight energy shifts [dashed lines in Fig. 1(d)] or changes in the linewidth. These effects (Δ_1 and Δ_2) are enough to break the symmetry between the states and lead to the generation of a FWM signal.

In Fig. 2, we show the results. Figure 2(a) shows the D_1 hyperfine states of both isotopes. Figures 2(b) and 2(c) correspond to double-quantum two-dimensional spectra obtained with collinearly ($HHHH$) and cross-linearly ($HVVH$) polarized excitation pulses. The diagonal peaks [along the line from (0, 0) to (10, 20) GHz] correspond to coupling between the same hyperfine energy levels of two atoms of the same isotopes (outer white dashed box for ^{87}Rb and inner white dashed box for ^{85}Rb). The off-diagonal peaks show coupling between different hyperfine energy levels of two atoms of the same as well as different isotopes. For instance, in Fig. 2(c), the peak at (9.0, 18.0) GHz corresponds to the coupling of two ^{87}Rb atoms that have the same (h) hyperfine resonance frequencies, whereas the peaks around (9.0, 11.2) GHz and (2.2, 11.2) correspond to coupling of two ^{87}Rb atoms with (h) and (g) hyperfine resonance frequencies, respectively. The peaks at (1.3, 4.2) GHz and (3.0 4.2) correspond to the coupling of ^{87}Rb and ^{85}Rb isotopes with (f) and (c) resonance frequencies, respectively. The similar analysis can be performed to identify all the peaks in double-quantum 2D spectra. The difference in strength for off-diagonal peaks between Figs. 2(b) and 2(c) we attribute to the difference in the number of magnetic sublevels (and their Clebsch-Gordon coefficients) that contribute in the generation of FWM signals for the $HHHH$ and $HVVH$ cases. For single-quantum 2D spectra, the difference is explained in Ref. [12]. We would like to note that we also performed a temperature dependence of 2D spectra. Below 75 °C the results were not reliable because of a low signal to noise ratio, whereas above 130 °C propagation effects (reabsorption) dominated and the peaks were obscured.

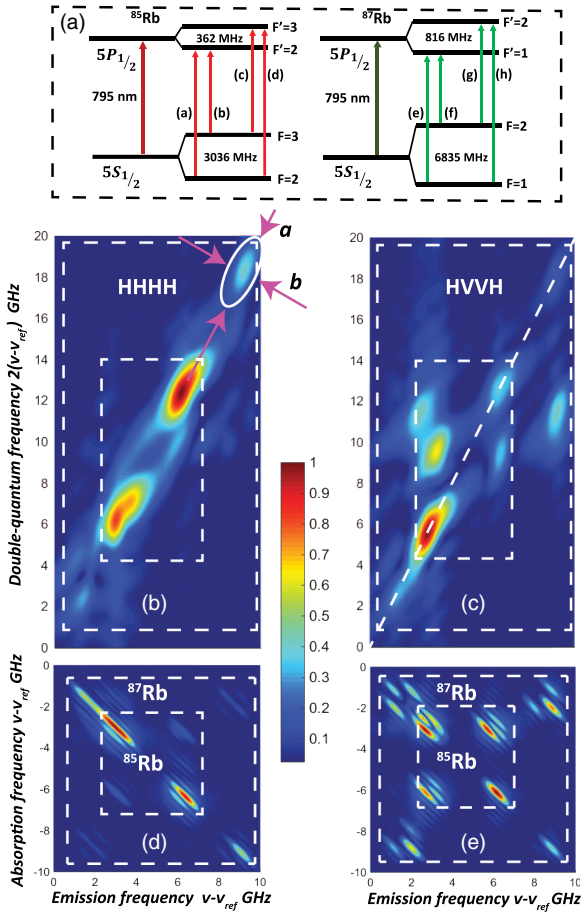

FIG. 2. (a) Energy level diagrams of D_1 hyperfine lines of ^{87}Rb and ^{85}Rb atoms. (b),(c) Double-quantum two-dimensional spectra acquired by collinearly and cross-linearly polarized excitation pulses. H, horizontal; V, vertical. (d),(e) Single-quantum two-dimensional spectra. The color scale shows the normalized signal magnitude, the reference frequency $\nu_{\mathrm{ref}} = 377.103$ THz.

Between 75 °C and 130 °C we did not observe changes on 2D spectra.

It is important to emphasize that double-quantum MDCS excels in isolating and identifying many-body interactions, because it allows the measurement of the FWM signal that is only due to the interactions. These interactions are, in most cases, not accessible with other methods, including single-quantum MDCS. To demonstrate this point, we compared double-quantum 2D spectra to single-quantum 2D spectra shown in Figs. 2(d) and 2(e) (taken by collinearly and cross-linearly polarized excitation pulses, respectively). The spectra were taken with the pulse ordering that leads to the formation of a photon echo (the complex conjugated pulse arrives first), which can be experimentally obtained by swapping the time order of the excitation pulses such that the AOM frequency-shifted pulse (A) arrives first [Fig. 1(a)]. The diagonal elements [along the (0,0) and $(10,-10)$ GHz line] correspond to FWM signals with the same absorption and emission hyperfine frequencies (a)–(h) for ^{87}Rb (outer white dashed box) and ^{85}Rb (inner white dashed box). They are diagonally elongated due to Doppler broadening. The cross-peaks, on the other hand, show all possible couplings between the hyperfine states within the same atom. In the photon echo excitation sequence, the FWM signal due to the couplings of two different atoms via the dipole-dipole interaction is nonzero. However, due to its weak strength compared to the FWM signal from individual atoms, the coupling peaks are not visible on 2D spectra. This shows that the single-quantum MDCS is not sensitive enough to probe the weak many-body interactions in atomic or molecular systems and measuring double-quantum spectra is required to isolate these interactions.

The double-quantum spectra show additional interesting behavior. The peaks are tilted and elongated along the diagonal line. The elongated peaks (along the diagonal) are expected for single-quantum spectra, because the pulses' time ordering produces a photon echo scheme. Double-quantum spectra, on the other hand, use a pulse time ordering that should not lead to a photon echo. The tilted and elongated line shapes on double-quantum spectra have previously been observed in molecules [28,29] and in static inhomogeneously broadened semiconductor materials [30] but have never been reported for Doppler-broadened systems. The elongation suggests that there is a correlation between the emission and double-quantum frequencies that gives insight about what velocity group of atoms participate in the generation of the FWM signal.

To demonstrate this point, we simulated a double-quantum 2D spectrum by solving the optical Bloch equations for two coupled two-level systems. Similar analysis has been performed by Tollerud and Davis [30]; however, in their simulation, an uncorrelated two-dimensional Gaussian function was used to include the inhomogeneous broadening for the coupled system. In our simulation, we model the broadening by using a generalized two-dimensional Gaussian function [31]:

$$f(x,y)=\frac{1}{2\pi\sigma_x\sigma_y\sqrt{1-\rho^2}}e^{-\{[(x-\mu_x)/\sigma_x]^2-2\rho[(x-\mu_x)/\sigma_x][(y-\mu_y)/\sigma_y]+[(y-\mu_y)/\sigma_y]^2\}/2(1-\rho^2)}, \quad (1)$$

where μ_x, μ_y, σ_x, and σ_y correspond to the centers and widths of two interacting Doppler-broadened resonances and ρ is a correlation parameter. $\rho=1$ implies that the resonances are perfectly correlated. For Doppler-broadened systems, this corresponds to the coupling of the resonances of those two atoms that have a zero relative velocity. $\rho=0$ corresponds to the coupling of resonances between two atoms that have any relative velocity.

In Fig. 3, we show the simulation results. Figures 3(a) and 3(b) show double-quantum 2D spectra for $\rho=0$ and $\rho=0.75$, respectively. In both cases, the peaks are diagonally elongated; however, quantitatively, they are very different. To give quantitative information, we measured the ellipticity of the peaks on 2D spectra:

$$E=\frac{a^2-b^2}{a^2+b^2}, \quad (2)$$

where a and b are the sizes of the ellipse along the major and minor axes, shown in Fig. 3(a) (upper right corner).

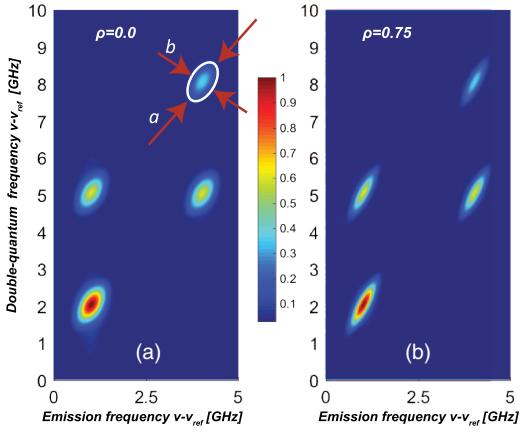

FIG. 3. Simulation results. (a) $\rho=0$, (b) $\rho=0.75$. ν_{ref} is the arbitrary optical frequency. The color scale shows the normalized signal magnitude.

For Fig. 3(a), we measured the ellipticity to be $E = 0.5$, whereas for Fig. 3(b), $E = 0.85$. This value is in very good agreement with the ellipticity of the measured peaks in Fig. 2(b) [for comparison, we chose an isolated peak that corresponds to the coupling of two ^{87}Rb atoms with (h) resonances in Fig. 2(b)]. $\rho = 0.75$ is a high correlation and indicates that the FWM signal is due to the coupled atoms with near zero relative velocities. A plausible explanation of the high correlation could be the fact that the dipole-dipole interaction is proportional to $(1/r^3)$, where r is the internuclear separation between the atoms. If two atoms have a nonzero relative velocity, then their internuclear separation changes during the time between the second and third excitation pulses (that is scanned over 1 ns). For high relative velocities, this could causes the dipole-dipole interaction to degrade rapidly $(1/r^3)$ and hence to decrease the strength of the FWM signal.

In conclusion, we have demonstrated the measurement of collective hyperfine resonances in a vapor of Rb atoms induced by the dipole-dipole interactions. We have identified the peaks corresponding to the couplings between the hyperfine levels of two atoms of the same and different isotopes. We have reported tilted and elongated peaks in double-quantum 2D coherent spectra for a Doppler-broadened system and explained the origin of the tilt in terms of the velocity group of atoms that participate in dipole-dipole interactions. The results shown here complement the studies of many-body interactions in atomic ensembles, and they provide important insight of the effects of thermal motion on dipole-dipole interactions. In addition, these results will impact research on photosynthesis and understanding the formation of homonuclear, heteronuclear, and exotic molecules.

The combination of single- and double-quantum spectra makes frequency-comb based multidimensional coherent spectroscopy an extremely powerful tool for obtaining complete and high-resolution spectroscopic information. This novel method now makes MDCS relevant for systems that have long dephasing rates. It allows the study of weak many-body (dipole-dipole) interactions in atomic and molecular (cold, Rydberg, and exotic) systems and color centers that are promising candidates for quantum computing.

The research is based upon work supported by the Office of the Director of National Intelligence (ODNI), Intelligence Advanced Research Projects Activity (IARPA), via Contract No. 2016-16041300005. The views and conclusions contained herein are those of the authors and should not be interpreted as necessarily representing the official policies or endorsements, either expressed or implied, of the ODNI, IARPA, or the U.S. Government. The U.S. Government is authorized to reproduce and distribute reprints for Governmental purposes notwithstanding any copyright annotation thereon. We thank Professor Paul Berman for helpful discussions and Christopher Smallwood and Eric Martin for comments on the manuscript.

*cundiff@umich.edu

[1] D. L. Andrews and A. A. Demidov, *Resonance Energy Transfer* (Wiley, New York, 1999).
[2] S. Ravets, H. Labuhn, D. Barredo, L. Beguin, T. Lahaye, and A. Browaeys, Nat. Phys. **10**, 914 (2014).
[3] E. Collini, C. Y. Wong, K. E. Wilk, P. M. G. Curmi, P. Brumer, and G. D. Scholes, Nature (London) **463**, 644 (2010).
[4] V. Bendkowsky, B. Butscher, J. Nipper, J. P. Shaffer, R. Low, and T. Pfau, Nature (London) **458**, 1005 (2009).
[5] A. Browaeys, D. Barredo, and T. Lahaye, J. Phys. B **49**, 152001 (2016).
[6] E. Urban, T. A. Johnson, T. Henage, L. Isenhower, D. D. Yavuz, T. G. Walker, and M. Saffman, Nat. Phys. **5**, 110 (2009).
[7] G. K. Brennen, C. M. Caves, P. S. Jessen, and I. H. Deutsch, Phys. Rev. Lett. **82**, 1060 (1999).
[8] S. Cundiff and S. Mukamel, Phys. Today **66**, No. 7, 44 (2013).
[9] P. Hamm and M. Zanni, *Concepts and Methods of 2D Infrared Spectroscopy* (Cambridge University Press, Cambridge, England, 2011).
[10] R. R. Ernst, G. Bodenhausen, and A. Wokaun, *Principles of Nuclear Magnetic Resonance in One and Two Dimensions* (Oxford University, New York, 1987).
[11] N. A. Kurnit, I. D. Abella, and S. Hartmann, Phys. Rev. Lett. **13**, 567 (1964).
[12] B. Lomsadze and S. T. Cundiff, Science **357**, 1389 (2017).
[13] L. Yang and S. Mukamel, Phys. Rev. Lett. **100**, 057402 (2008).
[14] L. Yang and S. Mukamel, Phys. Rev. B **77**, 075335 (2008).
[15] F. Gao, S. T. Cundiff, and H. Li, Opt. Lett. **41**, 2954 (2016).
[16] X. Dai, M. Richter, H. Li, A. D. Bristow, C. Falvo, S. Mukamel, and S. T. Cundiff, Phys. Rev. Lett. **108**, 193201 (2012).
[17] L. Bruder, M. Binz, and F. Stienkemeier, Phys. Rev. A **92**, 053412 (2015).
[18] S. Mukamel, J. Chem. Phys. **145**, 041102 (2016).
[19] B. Lomsadze and S. T. Cundiff, Sci. Rep. **7**, 14018 (2017).
[20] S. T. Cundiff and J. Ye, Rev. Mod. Phys. **75**, 325 (2003).
[21] I. Coddington, N. Newbury, and W. Swann, Optica **3**, 414 (2016).
[22] B. Lomsadze and S. T. Cundiff, Opt. Lett. **42**, 2346 (2017).
[23] J. Roy, J.-D. Deschênes, S. Potvin, and J. Genest, Opt. Express **20**, 21932 (2012).
[24] T. Ideguchi, A. Poisson, G. Guelachvili, T. W. Hänsch, and N. Picqué, Opt. Lett. **37**, 4847 (2012).
[25] T. Ideguchi, A. Poisson, G. Guelachvili, N. Picqué, and T. W. Hänsch, Nat. Commun. **5**, 3375 (2014).

[26] For clarity, we separated the first and second interactions, but in the experiment these interactions happen simultaneously.
[27] S. Mukamel, *Principles of Nonlinear Optical Spectroscopy* (Oxford University, New York, 1999).
[28] J. Kim, S. Mukamel, and G. D. Scholes, Acc. Chem. Res. **42**, 1375 (2009), pMID 19552412.
[29] A. Nemeth, F. Milota, T. Manal, T. Pullerits, J. Sperling, J. Hauer, H. F. Kauffmann, and N. Christensson, J. Chem. Phys. **133**, 094505 (2010).
[30] J. Tollerud and J. A. Davis, J. Opt. Soc. Am. B **33**, C108 (2016).
[31] S. T. Cundiff, Phys. Rev. A **49**, 3114 (1994).